Normal-state electronic structure in the heavily overdoped regime of $Bi_{1.74}Pb_{0.38}Sr_{1.88}CuO_{6+\delta}$ single-layer cuprate superconductors: An angle-resolved photoemission study

K. Yang,[1] B. P. Xie,[1] D. W. Shen,[1] J. F. Zhao,[1] H. W. Ou,[1] J. Wei,[1] S. Wang,[1] Y. H. Wang,[1] D. H. Lu,[2] R. H. He,[2] M. Arita,[3] S. Qiao,[3] A. Ino,[4] H. Namatame,[3] M. Taniguchi,[3,4] F. Q. Xu,[5] N. Kaneko,[6] H. Eisaki,[6] and D. L. Feng[1,*]

[1]*Department of Physics, Applied Surface Physics State Key Laboratory, and Synchrotron Radiation Research Center, Fudan University, Shanghai 200433, China*

[2]*Stanford Synchrotron Radiation Laboratory, Stanford University, Stanford, California 94305, USA*

[3]*Hiroshima Synchrotron Radiation Center, Hiroshima University, Higashi-Hiroshima, Hiroshima 739-8526, Japan*

[4]*Graduate School of Science, Hiroshima University, Higashi-hiroshima, Hiroshima 739-8526, Japan*

[5]*National Synchrotron Radiation Laboratory, University of Science & Technology of China, Hefei 230027, Anhui, China*

[6]*AIST, 1-1-1 Central 2, Umezono, Tsukuba, Ibaraki 305-8568, Japan*

(Received 21 February 2006; published 7 April 2006)

We explore the electronic structure in the heavily overdoped regime of the single-layer cuprate superconductor $Bi_{1.74}Pb_{0.38}Sr_{1.88}CuO_{6+\delta}$. We found that the nodal quasiparticle behavior is dominated mostly by phonons, while the antinodal quasiparticle line shape is dominated by spin fluctuations. Moreover, while long range spin fluctuations diminish at very high doping, the local magnetic fluctuations still dominate the quasiparticle dispersion, and the system exhibits a strange metal behavior in the entire overdoped regime.

DOI: 10.1103/PhysRevB.73.144507 PACS number(s): 74.72.Hs, 71.18.+y, 79.60.Bm

I. INTRODUCTION

The high-T_c cuprate superconductors (HTSC's) have been studied for almost 20 years.[1] Anomalous and complicated phenomenology in the underdoped regime of HTSC's such as pseudogaps,[2] resonant modes in spin fluctuation spectra,[3] and possible charge ordering,[4,5] have led to a broad spectrum of theoretical proposals from the very conventional BCS-type models[6] to the very exotic ones involving various gauge fields.[7] Recent angle-resolved photoemission spectroscopy (ARPES) experiments resolved kinks of the quasiparticle dispersions in both nodal and antinodal regions of the Brillouin zone.[8–13] Whether these kinks are originated from electron-phonon or electron-magnon interaction is currently debated.[9–14] Nevertheless, the role of phonons in high temperature superconductivity is being revisited.[15]

To date, most experimental studies have been focusing on the anomalous, and certainly interesting, underdoped regime. On the other hand, although to be validated by experiments, the overdoped half of the phase diagram, particularly the heavily overdoped regime, is considered to be a "normal" metal regime where correlations are negligible. The electronic structure in this regime was seldom studied.[16–20] To build a comprehensive picture of high temperature superconductivity, it is crucial to study the properties of the entire overdoped regime, particularly the heavily overdoped regime, where little data are available at this stage. By examining the overall picture, one hopefully can understand the complications in the HTSC phenomenology better and resolve some of the current controversies, and thus sort out properties that are essential for the high temperature superconductivity.

In this paper, we report a systematic ARPES study of the electronic structure in the heavily overdoped regime of HTSC's up to the extreme doping level where the superconductivity vanishes (referred as ultraoverdoped regime hereafter). Our data indicate that lattice effects dominate the nodal quasiparticle scattering, while the spin fluctuations dominate the antinodal region. Although long range spin fluctuations diminish at high doping together with the weakening superconductivity, the local antiferromagnetic fluctuations still dominate the quasiparticle dispersion, and correlations are still strong.

II. EXPERIMENT

High quality superstructure-free $Bi_{1.74}Pb_{0.38}Sr_{1.88}CuO_{6+\delta}$ (Pb-Bi2201) single crystals were grown by a floating-zone technique. Unlike $Bi_2Sr_2CaCu_2O_{8+\delta}$ (Bi2212), Pb-Bi2201 is a single-layer cuprate and can be doped into a much higher doping level. Through oxygen or argon annealing, we have prepared overdoped samples with superconducting phase transition temperatures T_c's (dopings) of 0 K (0.27), 5 K (0.26), 7 K (0.258), 10 K (0.252), 16 K (0.24), and 22 K (0.225), where the hole concentration x's are estimated based on the empirical formula $T_c = T_{c,opt}[1-82.6(x-0.16)^2]$,[21] and $T_{c,opt}=34$ K for Bi2201. For comparison, we also studied a Pb-free optimally doped Bi2201 ($T_c=34$ K, $x=0.16$). Transition widths of these samples are typically 1–2 K. Moreover, unlike $La_{2-x}Sr_xCuO_4$ (LSCO), the cleavage surface of Bi2201 is nonpolar and stable, suitable for angle-resolved photoemission studies. ARPES experiments were performed at the Beamline 5-4 of Stanford Synchrotron Radiation Laboratory (SSRL), and Beamline 9 of Hiroshima Synchrotron Radiation Center (HiSOR). Both beamlines are equipped with a Scienta SES200 electron analyzer, with a typical angular resolution of 0.3° and an energy resolution of 10 meV. If not specified, the data were taken at 10–15 K above T_c with 22.7 eV photons.

III. RESULTS AND DISCUSSION

We start with the examination of the nodal quasiparticle behavior. Figure 1(a) shows the nodal photoemission inten-

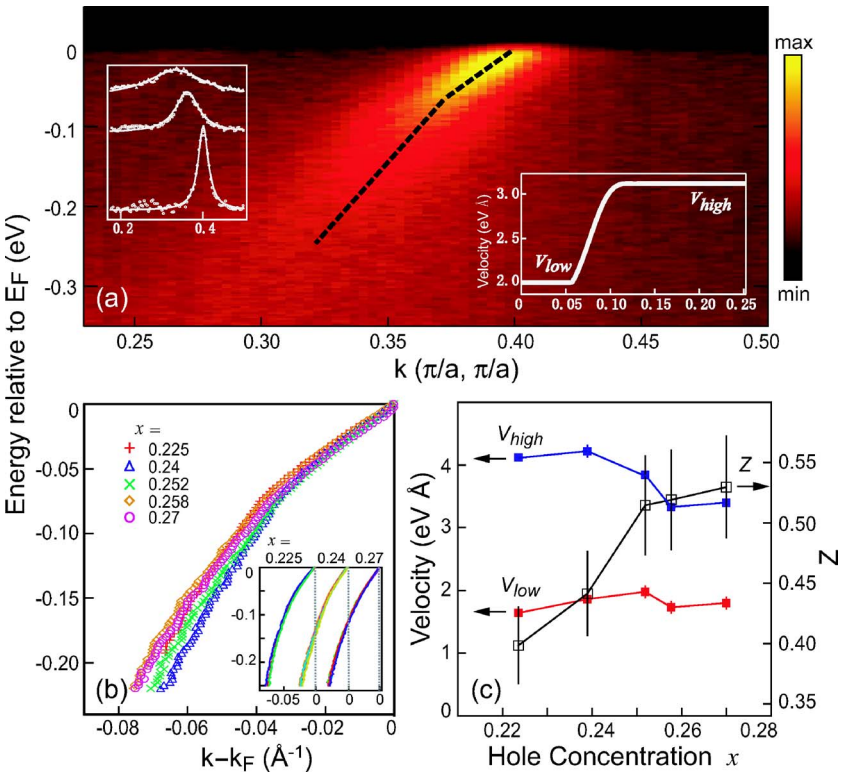

FIG. 1. (Color online) (a) Normal state photoemission intensity as a function of energy and nodal momentum for $x=0.26$. The inset on the left is MDC's at different binding energies that can fit well with a Lorentzian. The dispersion is extracted through the MDC analysis and illustrated as the thick dashed line. The inset on the right is the band velocity based on the dispersion, where it is a fixed value at low or high binding energies defined as V_{low} or V_{high}. (b) Dispersion extracted from the MDC analysis in the nodal direction for various doping levels. Inset: Dispersions for $x=0.225$ and $T=30$, 100, and 200 K; $x=0.24$ and $T=60$, 120, 190, and 250 K; and $x=0.27$ and $T=10$, 100, 150, 200, and 250 K. (c) V_{low}, V_{high} and $Z \equiv V_{low}/V_{high}$ as a function of doping.

sity map, where a kink in dispersion is clearly visible even for the $x=0.26$ high doping level.[9] As illustrated by the thick dashed line, one can extract the effective band velocities V_{high} and V_{low} for dispersions below and above the kink energy scale respectively [inset of Fig. 1(a)]. Dispersions and effective band velocities for various dopings are displayed in Figs. 1(b) and 1(c), respectively. Similar to the LSCO system,[22] V_{low} here is also almost doping independent, while V_{high} decreases slowly with increased doping. Recently, it has been shown that the coherent quasiparticle spectral weight Z can be estimated as V_{low}/V_{high} for cuprates,[23] which increases from 0.4 at $x=0.225$, to 0.53 at $x=0.27$ [see Fig. 1(c)]. These agree quite well with the calculations by Paramekanti *et al.*[24] At different temperatures [inset in Fig. 1(b)], the dispersion varies very little, indicating that Z does not decrease with rising temperature. Therefore, in the highly overdoped regime of Bi2201, we do not observe a coherent-incoherent transition with increasing temperature as a recent study of an overdoped Bi2212 claimed.[25]

Figure 2(a) compares the photoemission spectrum at a nodal Fermi crossing and that at $(\pi,0)$ for four different dopings ranging from the optimal doping level to an ultraoverdoped $T_c=0$ K sample. Remarkably, the $(\pi,0)$ spectrum sharpens up dramatically with increased doping, while the nodal spectral linewidth is quite doping independent. At very high doping, the $(\pi,0)$ spectrum appears to be even sharper than the nodal spectrum. The full width half maximum (FWHM) of these spectra are plotted in Fig. 2(b) as solid symbols. After removing the energy broadening from the finite energy resolution and angular resolution, which is significant in the nodal direction due to the fast dispersion,[26] one obtains the intrinsic energy width shown as open symbols. The scattering rate at $(\pi,0)$ almost decreases by a factor of 5 in a linear fashion, while the scattering of the nodal quasiparticles remains roughly constant. In the ultraoverdoped regime, the nodal and $(\pi,0)$ quasiparticles have the same linewidth, i.e., the scattering across the Fermi surface becomes isotropic.

Based on the above experimental observations, one can retrieve information on the interactions between electrons and bosons in the nodal and antinodal regions. In cuprates, the possible candidates for the bosons are phonons and spin excitations. For the nodal quasiparticles, the linewidth is almost doping independent, while Z increases with doping. This peculiar behavior resembles the photoemission spectrum of hydrogen molecules, where the vibration modes take the quasiparticle spectral weight from the main peak and redistribute it in multiple mode energies away without affecting the main peak linewidth.[8,27] In solids, as simulated in Figs. 2(d) and 2(e), it is only when electrons interact with *discrete* bosonic modes with frequencies larger than the original quasiparticle width, could the quasiparticle keep a fixed width while its spectral weight increases with a weakening coupling strength. A half-breathing phonon may be a candidate to explain our data; it was suggested to interact strongly with the nodal quasiparticles in the Bi2212 system.[9,14] Moreover, since phonon spectrum does not vary significantly with doping, the increasing screening of electron-phonon interactions can explain the moderate 30% increase of Z from $x=0.225$ to 0.27. On the other hand, we found that in Figs. 2(f)–2(i), because the spin excitation is a broad spectrum starting from zero frequency in the normal state,[29,30] its scattering with electrons causes the resulting spectral linewidth a large doping dependence. Furthermore, spin excitation spectral weights drop rapidly to a negligible level at high doping,[30] which is hard to count for the loss of 47% (i.e., $1-Z$) of the nodal coherent quasiparticle weight

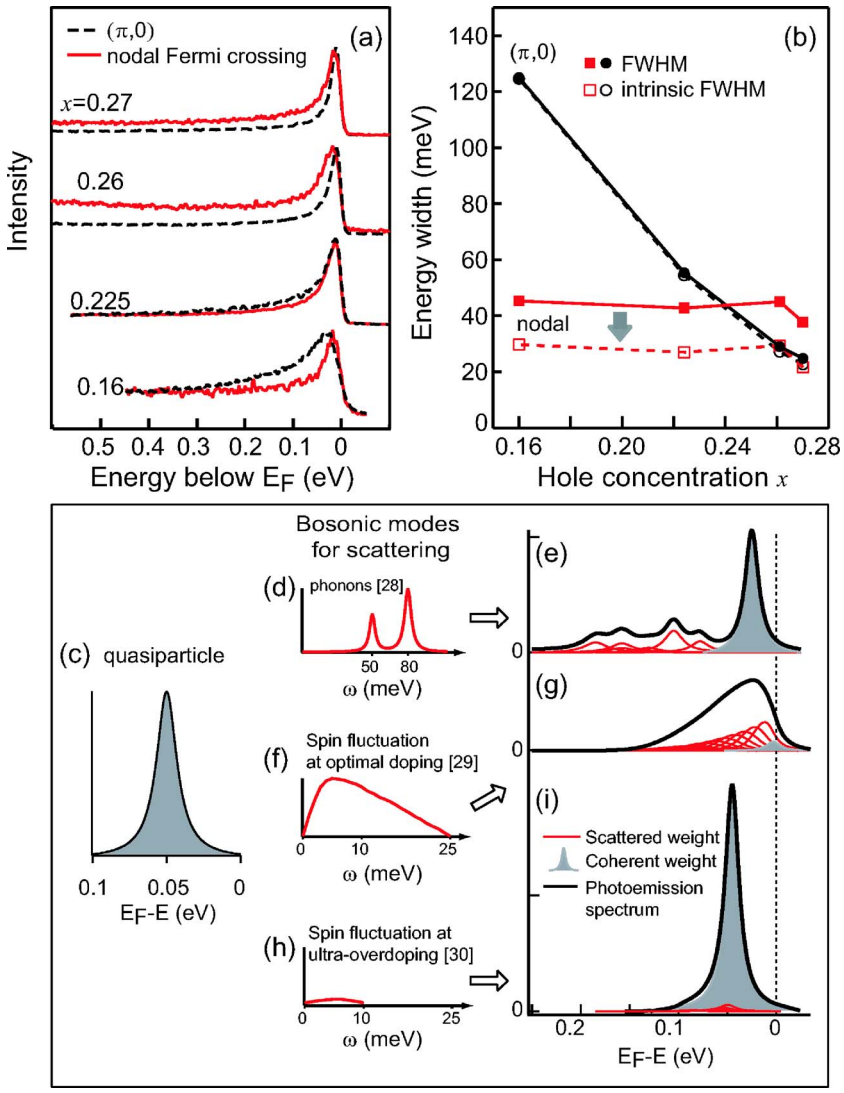

FIG. 2. (Color online) (a) The evolution of the photoemission spectral line shape of the Bi2201 system as a function of doping. Compared with the spectrum at nodal Fermi crossing (solid curves), the $(\pi,0)$ (dashed curves) gradually sharpens up with increased hole doping. (b) FWHM of the spectra in (a) are displayed in solid symbols, and the intrinsic FWHM after deducting the resolution effects are shown in empty symbols. (c)–(i) Numerical simulations of the effects of quasiparticle-bosonic mode interactions on photoemission line shape. When the original quasiparticle (c) is scattered multiple times by discrete optical phonon modes (d), or spin fluctuations at optimal doping (f), or at ultraoverdoping (h), the resulting photoemission line shapes are illustrated in (e), (g), and (i), respectively. Realistic parameters are implemented in the simulation. The intrinsic quasiparticle width is set to 20 meV; the multiple optical phonon modes in the relevant energy region are based on maximum entropy analysis results on Bi2201 spectra in Ref. 28; and the spin fluctuation spectra near (π,π) are taken from inelastic neutron scattering measurements in the normal state for optimally doped, (Ref. 29) and ultraoverdoped $T_c \sim 4.5$ K single layer LSCO systems (Ref. 30) since the data on Bi2201 are unavailable. The residual quasiparticle weight Z in (e) is set to 0.5, which restrains the scattering strength. The scattering strength in (g) is chosen so that the spectral linewidth is close to the experimental one after deducting a background. The relative strength between spin fluctuation intensities in (f) and (h) are based on an extrapolation of the doping dependence of maximum $\chi''(\omega)$ in Ref. 30, which in turn determines the scattered weight in (i).

for $x=0.27$. Therefore, these observations indicate that optical phonons may dominate the scattering of quasiparticles in the nodal region.

Contrary to the nodal case, the *continuously* fast decreasing $(\pi,0)$ linewidth with doping [Fig. 2(b)] can be explained by the simulation in Figs. 2(f)–2(i). The broad $(\pi,0)$ spectrum at optimal doping can be attributed to the strong scattering from the antiferromagnetic fluctuations near (π,π) [Fig. 2(g)].[29] Consistently, when spin fluctuations are significantly weaker in the ultraoverdoped regime as shown by recent neutron scattering data [Fig. 2(h)],[30] the spectral linewidth gradually recovers its original quasiparticles width [Fig. 2(i)], eventually resulting in an isotropic linewidth across the Fermi surface for $T_c \sim 0$ K. Therefore, the doping and momentum dependence of the quasiparticle lifetime indicate the dominant role of spin fluctuations to the antinodal quasiparticles. As for phonon effects in this region, the out-of-plane B_1g buckling phonon was suggested to interact strongly with the antinodal quasiparticles in bilayer systems due to the nonzero crystal field along the c axis at the CuO_2

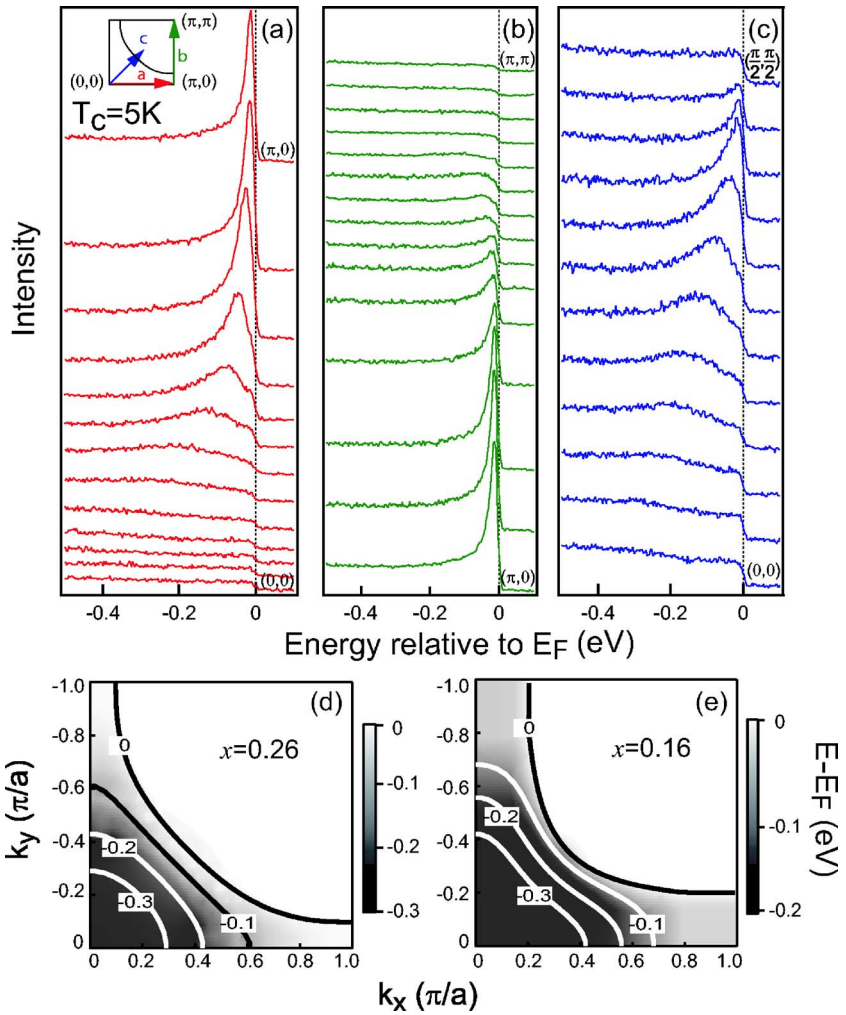

FIG. 3. (Color online) (a)–(c) Photoemission spectra along three high-symmetry lines as indicated in the inset of panel (a) for $x=0.26$. Data are taken at 12 K with a helium lamp. (d) and (e) image plots of dispersions extracted from the photoemission peak position of $x=0.26$ and $x=0.16$, respectively. The contour curves are the tight-binding fits to the dispersions.

planes.[13,14,31] However, for a single-layer Bi2201, the surroundings of the CuO_2 plane are symmetric, thus the crystal field induced electron-buckling phonon coupling is negligible in Bi2201.[31] For the in-plane half-breathing phonon, it has been suggested that it only interacts weakly with the electrons in the antinodal region.[14] However, we note that at ultraoverdoping, when spin fluctuations diminish, effects of other phonons might become relatively pronounced in the quasiparticle lineshape [not included in Fig. 2(i) for simplicity].

Having studied the nodal and $(\pi,0)$ quasiparticles, we now turn to the overall dispersion. Figures 3(a)–3(c) present the normal state ARPES spectra measured on the ultraoverdoped $x=0.26$ sample along the high-symmetry directions of the first Brillouin zone. Tracking the peak position of the spectrum, the quasiparticle dispersion is plotted in a false color in Fig. 3(d) for $x=0.26$ and 3(e) for $x=0.16$ for comparison, which shows that the overall dispersion energy scale is not very sensitive to doping. Moreover, we observed a hole-like Fermi surface even at the highest doping level. The data can be well fitted with an effective tight-binding model (shown as contour), $\varepsilon(k)=e_0-2t(\cos k_x+\cos k_y)-4t'\cos k_x\cos k_y-2t''(\cos 2k_x+\cos 2k_y)$.[32,33] We got the effective hopping parameters:

x	t (eV)	t' (eV)	t'' (eV)	e_0 (eV)
0.26	0.164(2)	−0.035(1)	0.015(1)	0.182(1)
0.16	0.130(5)	−0.010(3)	0.034(2)	0.062(2)

If the correlations at the ultraoverdoped regime were very weak, one would expect the effective hopping between nearest neighbors, t, to be much larger, close to 0.4 eV as estimated by band structure calculations. But the small t here clearly indicates that the dispersion energy scale is still of the exchange energy J. It is interesting to note that although the long range magnetic fluctuations are much reduced when approaching the ultraoverdoped regime, the local antiferromagnetic correlations still determine the hopping behavior of the holes. This is consistent with the recent numerical studies based on the $t-t'-t''-J$ model, showing that the dispersion of the centroid of the occupied state has a very small doping dependency.[34]

The highly overdoped system possesses both strong correlation and well-defined quasiparticle. The energy dependence of the nodal quasiparticle scattering rate, i.e., $\Delta E \equiv V \times \Delta k$ is plotted in Figs. 4(a) and 4(b) for two dopings, where V is the band velocity indicated in the inset of Fig. 1(a). The shaded regions correspond to the kink, which gives an upturn in a scattering rate due to electron-boson interactions, where

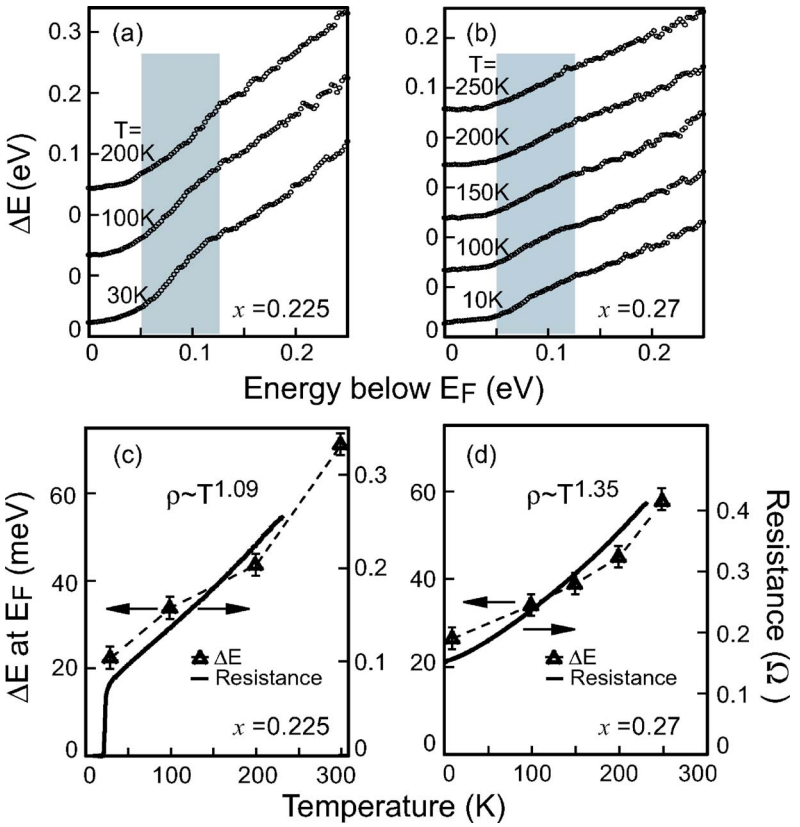

FIG. 4. (Color online) (a) and (b) Binding energy dependence of the quasiparticle inverse lifetime along the nodal direction for $x=0.225$, and 0.27, respectively. The shaded regions indicate kink effects in scattering. (c) and (d) Temperature dependence of the nodal quasiparticle inverse lifetime at E_F and resistance for $x=0.225$, and 0.27, respectively.

these bosons are most likely phonons as discussed above. The low energy region can be fitted with a power law function, $\Delta E \sim \omega^{\alpha}$, but α varies from 1 to 3, depending on the choice of the fitting of the energy window. Meanwhile, the high energy portion above the kink region is always linear. As a function of temperature, the in-plane resistance is plotted in Figs. 4(c) and 4(d) together with the nodal quasiparticle scattering rate at the Fermi energy. Close-to-linear behavior is observed for $x=0.225$, while for $x=0.27$, a superlinear temperature dependence is observed, $\rho \sim T$.[1,35] Similarly, early resistivity studies of ultraoverdoped $Tl_2Ba_2CuO_{6+\delta}$ have shown superlinear behavior as well.[35] These temperature dependence behavior and the interesting energy dependence indicate that the system is still a "strange metal" state in the ultraoverdoped regime.

The non-Fermi liquid behavior near the optimal doping was related to a possible quantum critical point in the vicinity.[36–38] The transition from a marginal Fermi liquid behavior toward a more Fermi-liquid-like behavior with a tuning of the doping does resemble the quantum critical phenomena observed in $Sr_3Ru_2O_7$ and $YbRh_2Si_2$.[39,40] Moreover, in various doping levels and temperatures that were sampled, we so far do not observe any abrupt change in the electronic structure that might be related to a first order transition, whether or not there is one or more quantum critical points that still need more decisive evidence.

IV. CONCLUSION

The nodal quasiparticles display many doping-insensitive properties such as the linewidth, v_{low}. We find them not affected by the long range magnetic fluctuations. Since nodal quasiparticles are responsible for many transport properties, our observations put strong constraints to theories of transport. For the antinodal region where the gap is the largest, the data suggest that long range magnetic fluctuations play an important role. The fact that d-wave superconductivity vanishes when the quasiparticle inverse lifetime across the Fermi surface becomes isotropic is very intriguing. Moreover, the quasiparticle dispersion is renormalized by roughly a factor of x from the bare band, indicative of that the local magnetic correlations are still surprisingly strong up to the ultraoverdoped regime.[41]

We conclude by pointing out that the ultraoverdoped regime exhibits many unconventional behaviors that may be fundamentally related to the mechanism of high temperature superconductivity, which calls for more comprehensive theory that could explain the phenomenology over the entire doping range.

ACKNOWLEDGMENTS

D.L.F. would like to thank Q. H. Wang, J. X. Li, and J. P. Hu for helpful discussions. This work was supported by the National Natural Science Foundation of China, by the 973 Project of the Science and Technology Ministry of China, and by the Shanghai Science and Technology Committee. Experiments at HSRL were supported by the Japan-China core university program; SSRL is operated by the DOE Office of BES, Divisions of Chemical Sciences and Material Sciences.

*Electronic address: dlfeng@fudan.edu.cn

[1] J. Orenstein and A. J. Millis, Science **288**, 468 (2000).
[2] T. Timusk and B. Statt, Rep. Prog. Phys. **62**, 61 (1999).
[3] Y. Sidis, S. Pailhes, B. Keimer, P. Bourges, C. Ulrich, and L. P. Regnault, Phys. Status Solidi B **241**, 1204 (2004).
[4] T. Hanaguri, C. Lupien, Y. Kohsaka, D.-H. Lee, M. Azuma, M. Takano, H. Takagi, and J. C. Davis, Nature (London) **430**, 1001 (2004).
[5] J. M. Tranquada, B. J. Sternlieb, J. D. Axe, Y. Nakamura, and S. Uchida, Nature (London) **375**, 561 (1995).
[6] Q. Chen, I. Kosztin, B. Jankó, and K. Levin, Phys. Rev. B **59**, 7083 (1999).
[7] P. A. Lee, N. Nagaosa, and X.-G. Wen, Rev. Mod. Phys. **78**, 17 (2006).
[8] A. Damascelli, Z. Hussain, and Z.-X. Shen, Rev. Mod. Phys. **75**, 473 (2003).
[9] A. Lanzara, P. V. Bogdanov, X. J. Zhou, S. A. Kellar, D. L. Feng, E. D. Lu, T. Yoshida, H. Eisaki, A. Fujimori, K. Kishio, J.-I. Shimoyama, T. Nodak, S. Uchidak, Z. Hussain, and Z.-X. Shen, Nature (London) **412**, 510 (2001).
[10] A. Kaminski, M. Randeria, J. C. Campuzano, M. R. Norman, H. Fretwell, J. Mesot, T. Sato, T. Takahashi, and K. Kadowaki, Phys. Rev. Lett. **86**, 1070 (2001).
[11] P. D. Johnson, T. Valla, A. V. Fedorov, Z. Yusof, B. O. Wells, Q. Li, A. R. Moodenbaugh, G. D. Gu, N. Koshizuka, C. Kendziora, Sha Jian, and D. G. Hinks, Phys. Rev. Lett. **87**, 177007 (2001).
[12] A. D. Gromko, A. V. Fedorov, Y.-D. Chuang, J. D. Koralek, Y. Aiura, Y. Yamaguchi, K. Oka, Yoichi Ando, and D. S. Dessau, Phys. Rev. B **68**, 174520 (2003).
[13] T. Cuk, F. Baumberger, D. H. Lu, N. Ingle, X. J. Zhou, H. Eisaki, N. Kaneko, Z. Hussain, T. P. Devereaux, N. Nagaosa, and Z.-X. Shen, Phys. Rev. Lett. **93**, 117003 (2004).
[14] T. P. Devereaux, T. Cuk, Z.-X. Shen, and N. Nagaosa, Phys. Rev. Lett. **93**, 117004 (2004).
[15] Z. X. Shen, A. Lanzara, S. Ishihara, and N. Nagaosa, Philos. Mag. B **82**, 1349 (2002).
[16] Z. M. Yusof, B. O. Wells, T. Valla, A. V. Fedorov, P. D. Johnson, Q. Li, C. Kendziora, Sha Jian, and D. G. Hinks, Phys. Rev. Lett. **88**, 167006 (2002).
[17] A. Ino, T. Mizokawa, K. Kobayashi, A. Fujimori, T. Sasagawa, T. Kimura, K. Kishio, K. Tamasaku, H. Eisaki, and S. Uchida, Phys. Rev. Lett. **81**, 2124 (1998).
[18] T. Sato, Y. Naitoh, T. Kamiyama, T. Takahashi, T. Yokoya, J. Mesot, A. Kaminski, H. Fretwell, J. C. Campuzano, H. Ding, I. Chong, T. Terashima, M. Takano, and K. Koxlowaki, Physica C **341**, 2091 (2000).
[19] T. Sato, T. Kamiyama, S. Nishina, T. Takahashi, I. Chong, T. Terashima, and M. Takano, Physica C **364**, 590 (2001).
[20] M. Plate, J. D. F. Mottershead, I. S. Elfimov, D. C. Peets, Ruixing Liang, D. A. Bonn, W. N. Hardy, S. Chiuzbaian, M. Falub, M. Shi, L. Patthey, and A. Damascelli, Phys. Rev. Lett. **95**, 077001 (2005).
[21] M. R. Presland, J. L. Tallon, R. G. Buckley, R. S. Liu, and N. E. Flower, Physica C **176**, 95 (1991).
[22] X. J. Zhou, T. Yoshida, A. Lanzara, P. V. Bogdanov, S. A. Kellar, K. M. Shen, W. L. Yang, F. Ronning, T. Sasagawa, T. Kakeshita, T. Noda, H. Eisaki, S. Uchida, C. T. Lin, F. Zhou, J. W. Xiong, W. X. Ti, Z. X. Zhao, A. Fujimori, Z. Hussain, and Z.-X. Shen, Nature (London) **423**, 398 (2003).
[23] M. Randeria, A. Paramekanti, and N. Trivedi, Phys. Rev. B **69**, 144509 (2004).
[24] A. Paramekanti, M. Randeria, and N. Trivedi, Phys. Rev. Lett. **87**, 217002 (2001).
[25] A. Kaminski, S. Rosenkranz, H. M. Fretwell, Z. Z. Li, H. Raffy, M. Randeria, M. R. Norman, and J. C. Campuzano, Phys. Rev. Lett. **90**, 207003 (2003).
[26] Linewidth broadening of the finite momentum resolution is in the order of $\Delta k \times v_F$, where Δk is the momentum resolution and v_F is Fermi velocity.
[27] D. W. Turner, A. D. Baker, C. Baker, and C. R. Brundle, *Molecular Photoelectron Spectroscopy* (Wiley, New York, 1970).
[28] W. Meevasana, N. J. C. Ingle, D. H. Lu, J. R. Shi, F. Baumberger, K. M. Shen, W. S. Lee, T. Cuk, H. Eisaki, T. P. Devereaux, N. Nagaosa, J. Zaanen, and Z.-X. Shen, cond-mat/0602508 (unpublished).
[29] G. Aéppli, T. E. Mason, S. M. Hayden, H. A. Mook, and J. Kulda, Science **278**, 1432 (1997).
[30] S. Wakimoto, H. Zhang, K. Yamada, I. Swainson, Hyunkyung Kim, and R. J. Birgeneau, Phys. Rev. Lett. **92**, 217004 (2004).
[31] T. P. Devereaux, A. Virosztek, and A. Zawadowski, Phys. Rev. B **51**, 505 (1995).
[32] M. R. Norman, M. Randeria, H. Ding, and J. C. Campuzano, Phys. Rev. B **52**, 615 (1995).
[33] A. I. Liechtenstein, O. Gunnarsson, O. K. Andersen, and R. M. Martin, Phys. Rev. B **54**, 12505 (1996).
[34] T. Tohyama, Phys. Rev. B **70**, 174517 (2004).
[35] A. P. Mackenzie, S. R. Julian, G. G. Lonzarich, A. Carrington, S. D. Hughes, R. S. Liu, and D. C. Sinclair, Phys. Rev. Lett. **71**, 1238 (1993); C. Proust, E. Boaknin, R. W. Hill, L. Taillefer, and A. P. Mackenzie, *ibid.* **89**, 147003 (2002).
[36] T. Valla, A. V. Fedorov, P. D. Johnson, B. O. Wells, S. L. Hulbert, Q. Li, G. D. Gu, and N. Koshizuka, Science **285**, 2110 (1999).
[37] D. van der Marel, H. J. A. Molegraaf, J. Zaanen, Z. Nussinov, F. Carbone, A. Damascelli, H. Eisaki, M. Greven, P. H. Kes, and M. Li, Nature (London) **425**, 271 (2003).
[38] S. Sachdev, Science **288**, 475 (2000).
[39] S. A. Grigera, R. S. Perry, A. J. SchoTeld, M. Chiao, S. R. Julian, G. G. Lonzarich, S. I. Ikeda, Y. Maeno, A. J. Millis, and A. P. Mackenzie, Science **294**, 329 (2001).
[40] J. Custers, P. Gegenwart, H. Wilhelm, K. Neumaier, Y. Tokiwa, O. Trovarelli, C. Geibel, F. Steglich, C. Pepin, and P. Coleman, Nature (London) **424**, 524 (2003).
[41] P. W. Anderson, P. A. Lee, M. Randeria, T. M. Rice, N. Trivedi, and F. C. Zhang, J. Phys.: Condens. Matter **16**, R755 (2004); F. C. Zhang, C. Gros, T. M. Rice, and H. Shiba, Supercond. Sci. Technol. **1**, 36 (1988); Q. H. Wang, Z. D. Wang, Y. Chen, and F. C. Zhang, cond-mat/0506712 (unpublished).